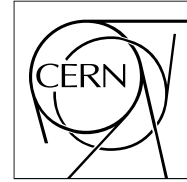


The Compact Muon Solenoid Experiment
Analysis Note

The content of this note is intended for CMS internal use and distribution only



December 29, 2007

Performance of the SIS Cone Jet Clustering Algorithm

A. Bhatti

The Rockefeller University, New York NY 10021

F. Chlebana, R. Harris, K. Kousouris

Fermilab

Z. Qi, M. Zielinski

University of Rochester

F. Ratnikov

University of Maryland

N. Varelas, C. Dragoiu

University of Illinois

M. Jha

University of Dehli

P. Kurt, H. Topakli

University of Cukurova

G. Dissertori

ETH Zurich

P. Schieferdecker

CERN

Abstract

We compare the performance of the Seedless Infrared Safe Cone (SIS Cone) jet clustering algorithm to that of the Midpoint algorithm. It is shown that reconstructed quantities are similar for the two algorithms and that they have similar performance for multijet processes such as top production. The SIS Cone algorithm does not have the problem of being infrared unsafe and does not leave unclustered

energy and is preferred by theorists. SISCone has been fully integrated into the CMSSW framework. We propose that SISCone be adopted as the default cone based jet clustering algorithm for CMS.

1 Introduction

The Standard Model describes hard interactions between partons. Partons which are not observable, manifest themselves through hadronization as stable particles which can then be detected in tracking chambers and calorimeters. Theory and modeling describes the interaction between constituent partons of the proton and the subsequent showering into stable particles. In addition to the hard interaction effects such as the underlying event and multiple interactions which will change the observable energy flow also have to be modeled. The evolution of a jet from the hard interaction to the observed energy deposits is shown schematically in Figure 1.

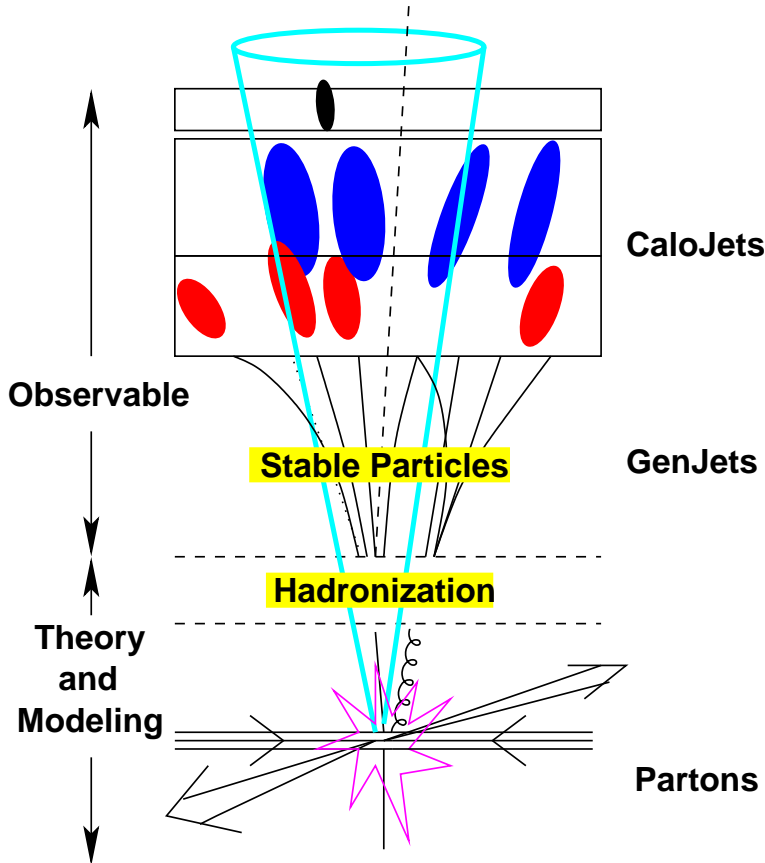


Figure 1: Evolution of a jet

Jet algorithms cluster energy deposits in the calorimeter or more generally four-vectors. A successful jet algorithm will provide a good correspondence between the first few orders of perturbation theory and the hadron level. Traditionally, jets have been defined using cone-based clustering algorithms which search for stable cones around the direction of significant energy flow. The steps of a typical cone-based algorithms are shown in Figure 2. Initially, cones are defined using the highest E_T tower (or four-vector) and the summed four-vector is calculated for all towers within the cone resulting in a proto-jet. The procedure is repeated until a stable proto-jet is found such that the proto-jets's four-vector coincides with the sum of the four-vectors of all the particles within the cone. Once the set of stable proto-jets is found, a splitting/merging procedure is applied to ensure that particles that are in the overlap region of the cones will end up in only one jet.

Cone algorithms that consider every tower as the starting direction for the initial cone have taken a prohibitively long time to execute. In order to reduce the computation time, a subset of four-vectors, referred to as “seeds”, is used. Two types of problems can arise when using seeds as starting points in cone algorithms. First, if a p_T cut is applied to the particles used as seeds, then the procedure becomes co-linearly unsafe and you can get a different set of jets at the calorimeter level or hadron level. Secondly, if any particle can act as a seed, then it is possible that the addition of a soft particle can lead to a new stable cone configuration making the result sensitive to the hadronization modeling and again yielding different jet configurations. These two effects are illustrated in Figure 3 and Figure 4.

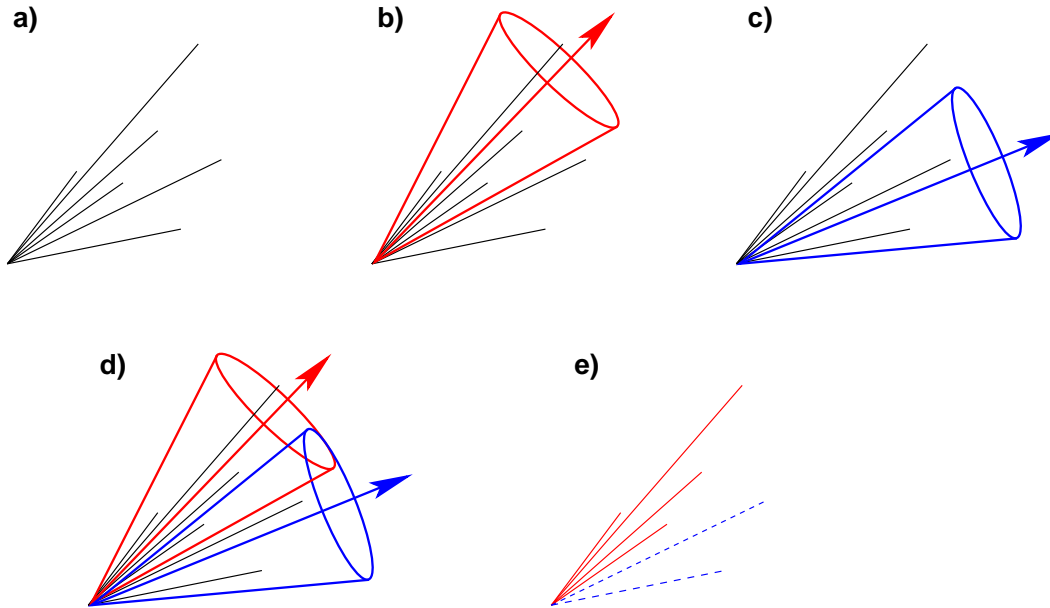


Figure 2: Steps in a jet clustering algorithm. a) Starting from an ordered list of four-vectors. b) and c) Stable cones are found. d) A splitting/merging algorithm is applied so that any four-vectors within the overlap of cones is assigned to a single jet. e) We end up with a final list of jets.

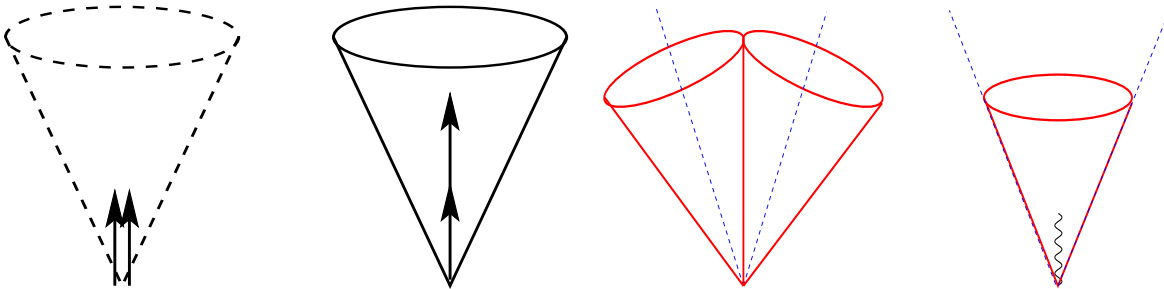


Figure 3: Collinear unsafe. Changing the p_T cut used for the seeds can lead to different stable cone configurations.

Figure 4: Infrared unstable. The addition of a soft particle can lead to new stable jet configurations.

It was attempted to solve the infrared safety issue by introducing additional seeds between the initial set of seeds. This procedure, coded in the MidPoint algorithm [3], was later shown to only delay the problem of infrared safety to the next order of the perturbative calculation [1]. Table 1, extracted from Reference [1], lists some processes together with the order at which jets are missed. As higher order calculations become available it will be necessary to use jet algorithms that are not sensitive to these problems.

Recently the Seedless Infrared Safe Cone (SIS Cone) [1] algorithm was developed which significantly improved the computation time allowing for all towers to be used as seeds. SIS Cone is both infrared and collinear safe and avoids some of the problems seen with previously used cone-based algorithms.

In addition to cone based jet algorithms there are clustering algorithms based on sequential recombination such as k_T , Jade, and Cambridge/Aachen [4]. The k_T algorithm merges pairs of four-vectors in order of increasing relative transverse momentum. The procedure is repeated until some stopping requirement is achieved, typically the distance between adjacent “jets” is greater than some value. These algorithms are infrared and collinear safe, have no artificial parameters, does not have “dark towers”, and can be applied equally well to both data and theory. One feature of these algorithms is that the jet area is ill defined making the subtraction of underlying event more difficult. Initial implementations of these algorithms were also very CPU intensive making them impractical to use. A faster implementation of the k_T algorithm, referred to as FastJet, is now available [5] and has been implemented

Table 1: Summary of the order at which stable cones are missed in various processes, taken from Reference [1]

Observable	1st miss cone at	Last meaningful order
Inclusive jet cross section	NNLO	NLO
W/Z/H + 1 jet cross section	NNLO	NLO
3 jet cross section	NLO	LO
W/Z/H + 2 jet cross section	NLO	LO
jet masses in 3 jets, W/Z/H + 2 jets	LO	none

within the CMSSW framework. In general cone based algorithms and sequential recombination algorithms will be sensitive to different effects and having both types of algorithms available allow for important cross checks.

In this note we compare the performance of SIS Cone with that of MidPoint. As will be shown, the performance of the two algorithms are similar and we propose that SIS Cone replace MidPoint as the default cone-based jet algorithm used by CMS.

1.1 MidPoint

The Midpoint algorithm first orders the list of four-vectors in p_T . A set of proto-jets is found starting from a set of four-vectors with $p_T > 1\text{GeV}$. In order to reduce the sensitivity to soft radiation, a list of seeds is added at the midpoint between the initial list of proto-jets. The number of iterations used when determining a stable proto-jet is limited to 100. Once a set of stable proto-jets is found a splitting/merging procedure is then applied. The splitting merging step specifies how to split or merge proto-jets that have overlapping four-vectors. The procedure starts with the highest p_T proto-jet. Proto-jets that share a p_T fraction, $f \geq .75$ will be merged. Proto-jets having an overlap fraction $f < .75$ are split. The overlapping four-vectors are assigned to the proto-jet that is closest in $\eta - \phi$. The list of proto-jets is reordered after each splitting/merging step, proto-jets which are split are moved down in the list, while proto-jets which are merged are moved up.

It has been shown that the addition of seeds at the midpoint between proto-jets only postpones the ‘‘infrared unsafe’’ problem to the next level of calculation.

1.2 SIS Cone

The Seedless Infrared-Safe Cone (SIS Cone) jet algorithm [1] is infrared safe and the absence of a R_{sep} provides a more direct correspondence between the parton and hadron level jets. The source code is maintained in Hep-Forge [2] which has a detector independent interface ensuring that the same clustering algorithm is applied by different experiments which facilitates comparisons.

2 Comparison

In this section we compare the performance of SIS Cone with MidPoint. Unless otherwise noted, the comparisons were done using the CMSSW152-based sample produced in Summer07 consisting of one million QCD dijet monte carlo events. The sample was generated in 21 PTHAT bins in order to provide sufficient statistics at high p_T .

2.1 Timing

The SIS Cone algorithm has reduced the computation time from N^2N to $N^2\ln N$, where N is the number of four-vectors being clustered. The external package FastJet has been interfaced to the CMSSW framework and calling the different clustering algorithms is done through a standard interface. Tests were done comparing the execution times of several clustering algorithms available at CMS using QCD MC samples with p_T in the ranges 30-50, 50-80, 80-120, and 3000-3500. The results are summarized in Figure 5. The execution time as a function of the number of towers is shown in Figure 6. The tests were done using FastJet v.2.1.0, SIS Cone v.1.1.1, and CMSSW 1.7.1 and run on a desktop computer with a 3GHz Xeon processor.

2.2 Jet Energy Corrections

Currently available jet corrections are based on the procedure outlined in Reference [6]. The jet correction has been determined using a QCD MC sample of about one million events generated using CMSSW 1.5.2. The jet

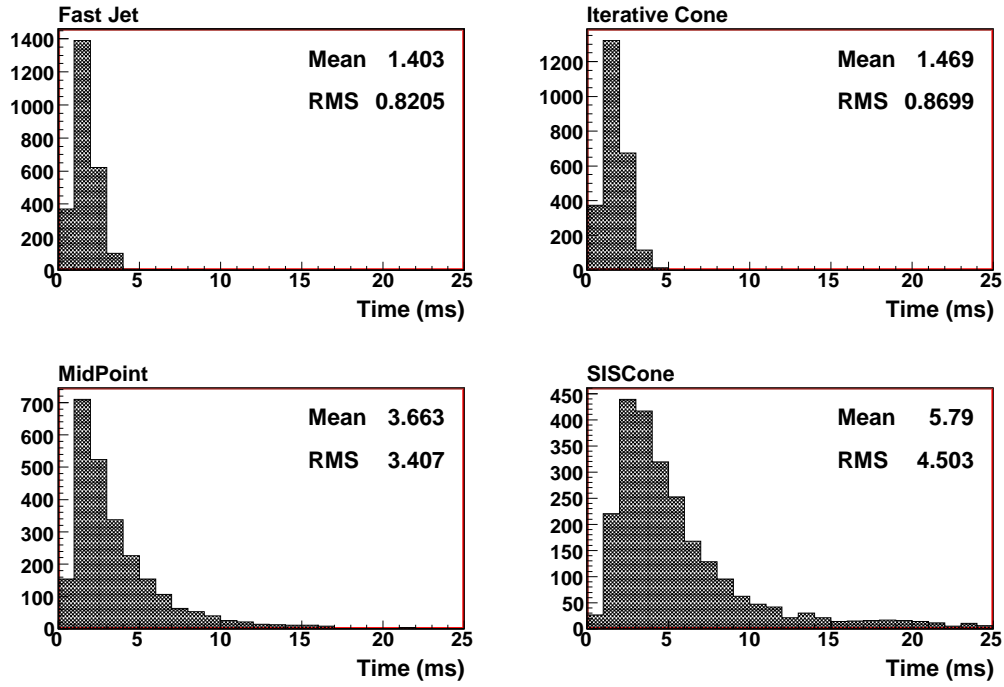


Figure 5: Execution time of several clustering algorithms available in the CMS software framework including FastJet (Kt), Iterative Cone, MidPoint, and SIScone.

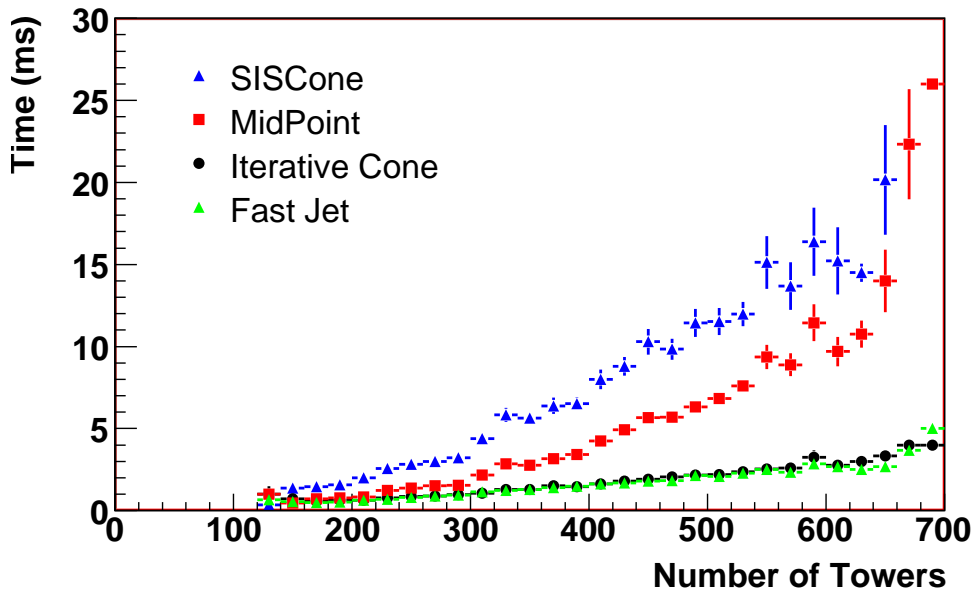


Figure 6: Execution time of several clustering algorithms available in the CMS software framework including MidPoint, SIScone, IterativeCone, and kT clustering.

response,

$$\text{Response} = \frac{E_T^{\text{Calo}}}{E_T^{\text{Gem}}}, \quad (1)$$

is defined as the ratio of reconstructed (Calo) jet E_T to that of the hadron level (Gen) jet E_T . Reconstructed (Calo) jets are uniquely matched to Generated jets by finding the closest pair in $\Delta R = \sqrt{\delta\eta^2 + \delta\phi^2}$ with the requirement that $\Delta R < 0.25$. The response distributions are made using all jets found in the event and bins in E_T and η in the interval $|\eta| < 5$. In the current version of the corrections, it is assumed that the detector is symmetric in η and no attempt was made to smooth the response when going across the η boundaries.

The jet response is binned in E_T and fit to a Gaussian. The mean values are parameterized as a function of E_T for 16 rapidity bins. The response for both SISCone and MidPoint as a function of the jet E_T is shown in Figure 7. The top row of plots are for cone=0.5 while the bottom row is for cone=0.7. The response is shown separately for one bin in the Barrel, Endcap, and Forward region. The jet correction is then provided as a function of the jet (detector) rapidity and jet E_T . Figure 7 compares the correction factor for SISCone and MidPoint in different η regions. The correction for SISCone and MidPoint similar over most of the E_T and η region. For lower E_T values and for the higher η region the correction factors start to deviate.

We do not expect that the response of different jet clustering algorithms to be the same, but we should be able to obtain the same level of correction for the different algorithms. The result of applying the jet corrections to SISCone jets is shown in Figure 9. The ‘‘closure plots’’ tests the correction by applying the correction derived from the QCD MC sample. The corrections are good to within about 1% for jets with $E_T > 30\text{GeV}$. work well for jets with $E_T > 30\text{GeV}$.

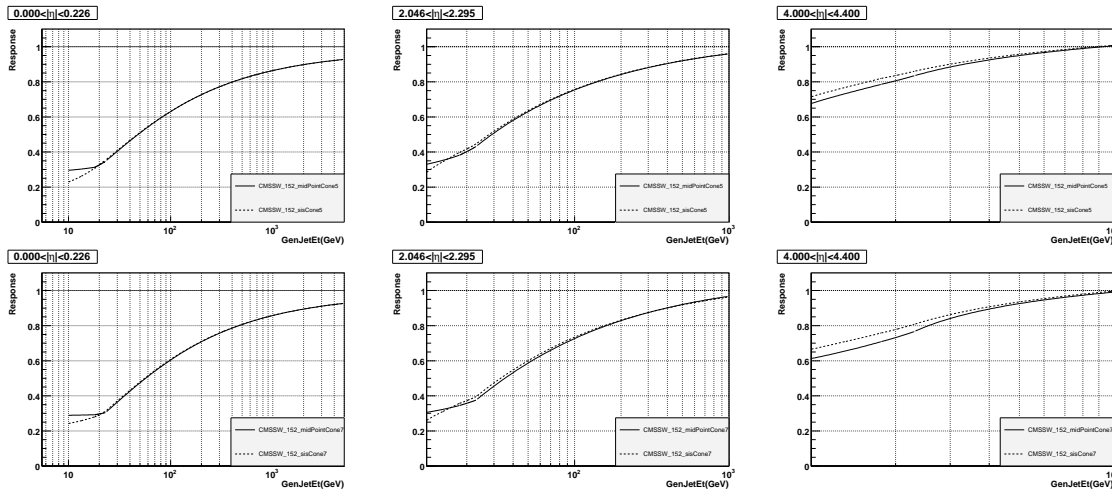


Figure 7: Jet response as a function of the jet E_T for MidPoint and SISCone. The top row shows the response for cone=0.5 and the bottom row is for cone=0.7. The response is shown for the Barrel (left column), Endcap (middle column), and the Forward (right column) regions.

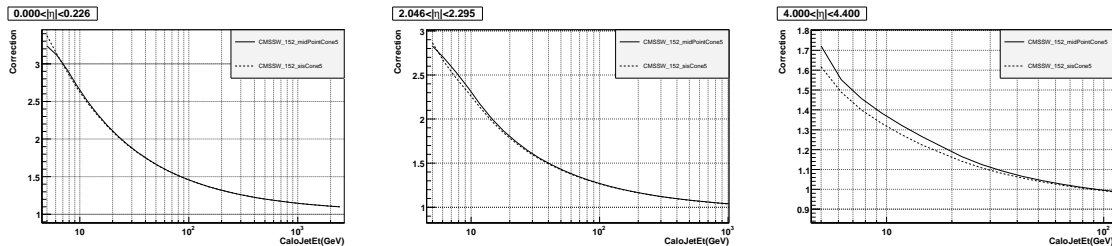


Figure 8: Comparison of the correction factor for SISCone and MidPoint as a function of the jet E_T . Three separate η bins are shown in the Barrel (left column), Endcap (middle column), and the Forward (right column) regions.

2.3 Jet Position Resolution

In order to determine the position resolution, Gen jets are matched with Calo jets using $\Delta R < 0.3$. The distribution of $\Delta\phi = \phi_{calo} - \phi_{gen}$ and $\Delta\eta = |\eta_{calo} - \eta_{gen}|$ is then plotted in p_T bins and fit to a Gaussian over the range (mean

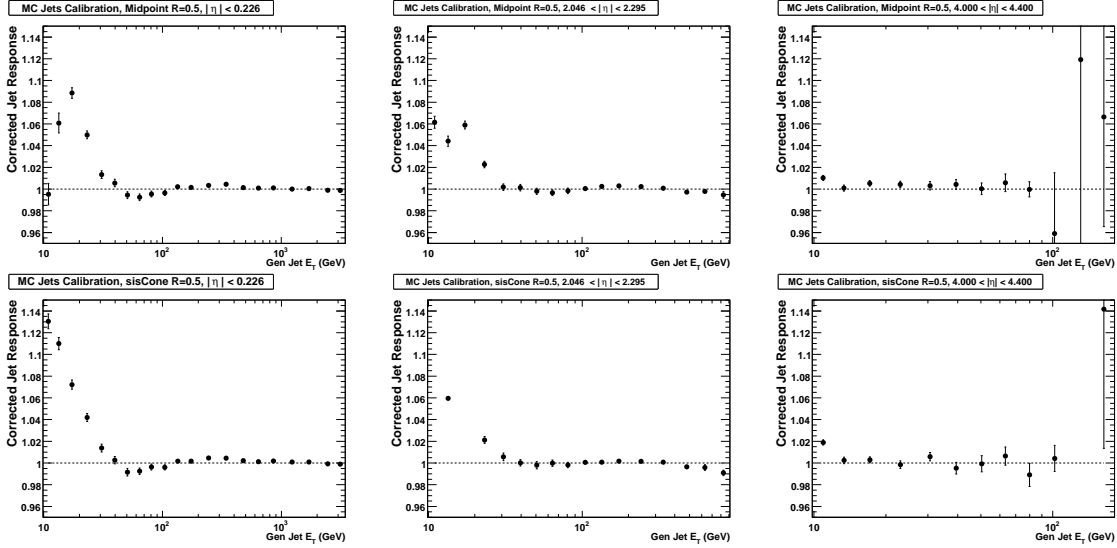


Figure 9: The corrected jet response shown as a function of E_T . The top row Three separate η bins are shown in the Barrel (left column), Endcap (middle column), and the Forward (right column) regions.

- $1.5 \cdot \text{RMS}$, mean + $1.5 \cdot \text{RMS}$). The resolutions are fit to the function shown in Equation 2.

$$\text{Resolution} = \frac{a}{E_T} = \oplus \frac{b}{\sqrt{E_T}} \oplus c \quad (2)$$

The η resolutions for SIScone and MidPoint are shown in Figure 10. The top row shows the results for a cone = 0.5 and the bottom row shows the results for a cone = 0.7. Different η bins are shown in the three columns. Similar results are shown for the ϕ resolution in Figure 11.

Both SIScone and MidPoint are in good agreement.

2.4 Energy Resolution of Corrected Jets

The jet energy resolution is defined as

$$\text{Resolution} = \frac{\sigma(E_T^{rec}/E_T^{gen})}{\langle E_T^{rec}/E_T^{gen} \rangle}. \quad (3)$$

Equation 3 is a measure of how well the reconstruction algorithm is able to reproduce the visible energy flow. Additional resolution effects arise from the hadronization process of going from the parton level to stable particles. The jet energy resolution is shown for the two leading jets in different η bins in Figure 12.

2.5 Unclustered Energy

In some cases the MidPoint algorithm will leave towers unassigned to a jet. These unclustered towers can have a significant E_T as is illustrated in Figure 14. The left plot shows the total E_T of all clustered towers in the jets. The middle plot shows the total E_T of the unclustered towers. A requirement of $E_T > 0.5$ was placed on the towers. The right plot shows the E_T distribution of unclustered towers. For k_T and SIScone there are no unclustered high E_T towers, while for the MidPoint case there are unclustered towers with $E_T \sim 45\text{GeV}$.

2.6 Reconstruction Efficiencies

The jet reconstruction efficiency is defined as the fraction of the Gen jets matched to Calo jets with a matching requirement of $\Delta R < 0.3$. Figure 15 shows ΔR for jets with $p_T > 15\text{GeV}$ while Figure 16 shows ΔR for jets with $p_T > 40\text{GeV}$. The matching requirement works well for jets with $p_T > 50\text{GeV}$. For lower p_T the jet position resolution is worse and it is necessary to use $\Delta R < 0.5$.

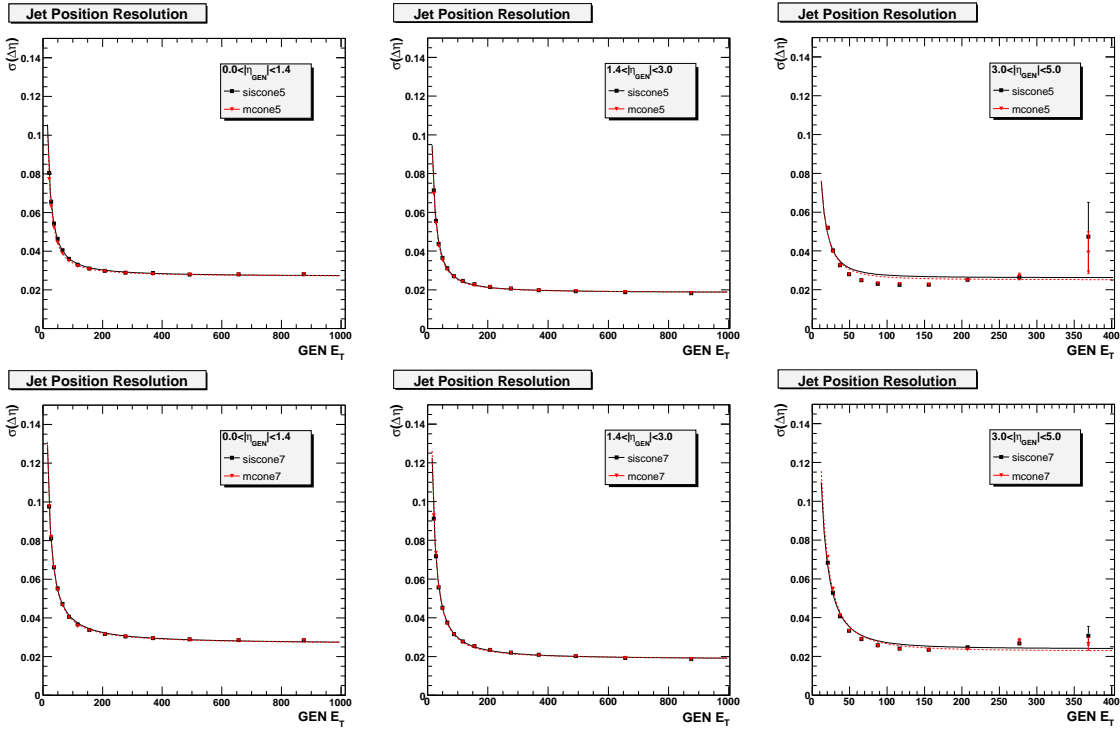


Figure 10: The jet η resolution for MidPoint and SISConic. The top row is for jets with a cone size of 0.5 and the bottom row is for jets with a cone size of 0.7. The different columns show the results for different η bins; $|\eta| < 1.4$, $1.4 < |\eta| < 3.0$, and $3.0 < |\eta| < 5.0$.

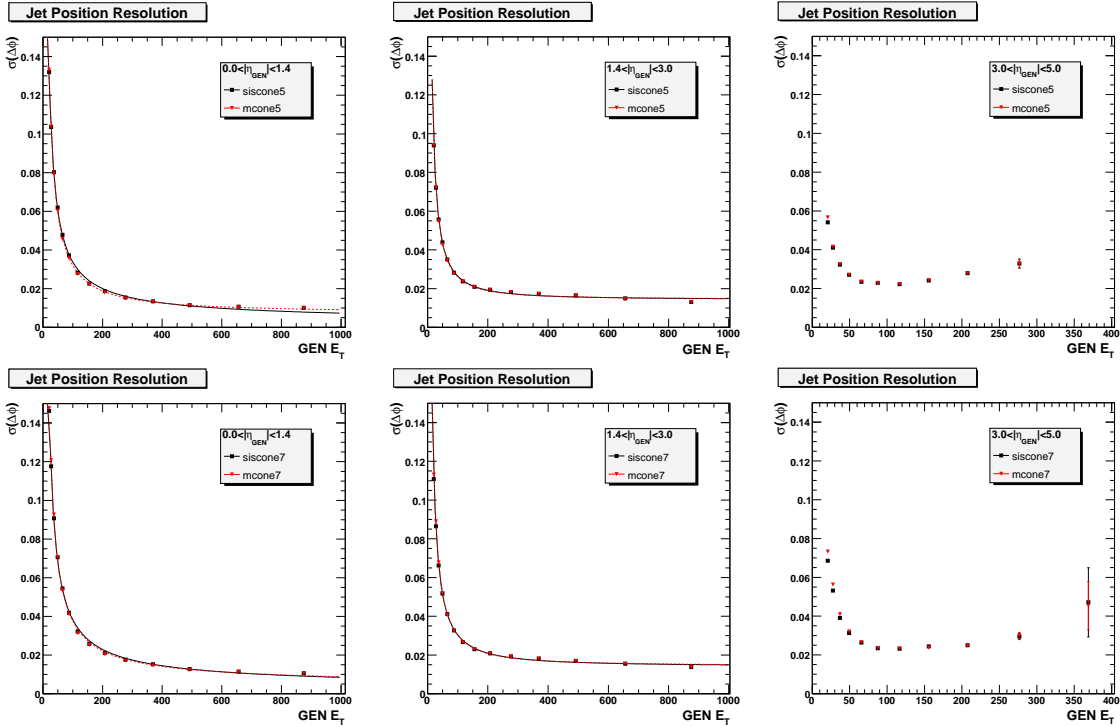


Figure 11: The jet ϕ resolution for MidPoint and SISConic. The top row is for jets with a cone size of 0.5 and the bottom row is for jets with a cone size of 0.7. The different columns show the results for different η bins; $|\eta| < 1.4$, $1.4 < |\eta| < 3.0$, and $3.0 < |\eta| < 5.0$.

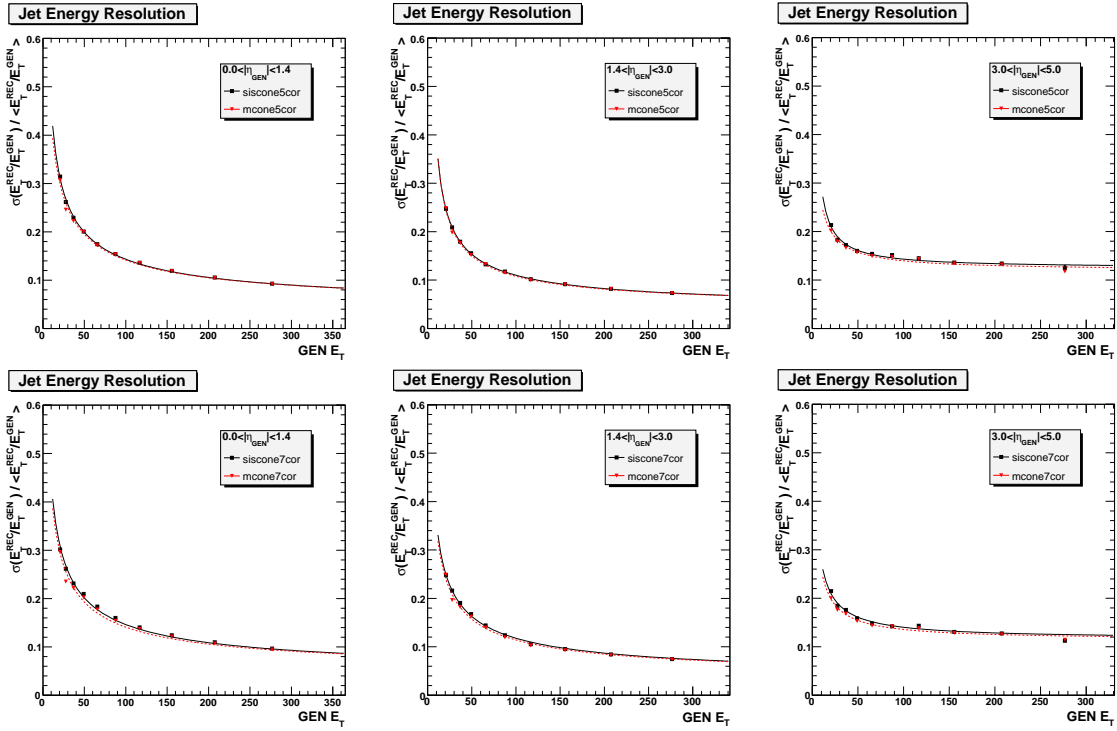


Figure 12: Jet E_T resolution of MidPoint and SIScone for the two leading jets. The top row shows the resolution for jets with a cone of 0.5 and the bottom row is for cone = 0.7. The different columns show the results for different η bins; $|\eta| < 1.4$, $1.4 < |\eta| < 3.0$, and $3.0 < |\eta| < 5.0$.

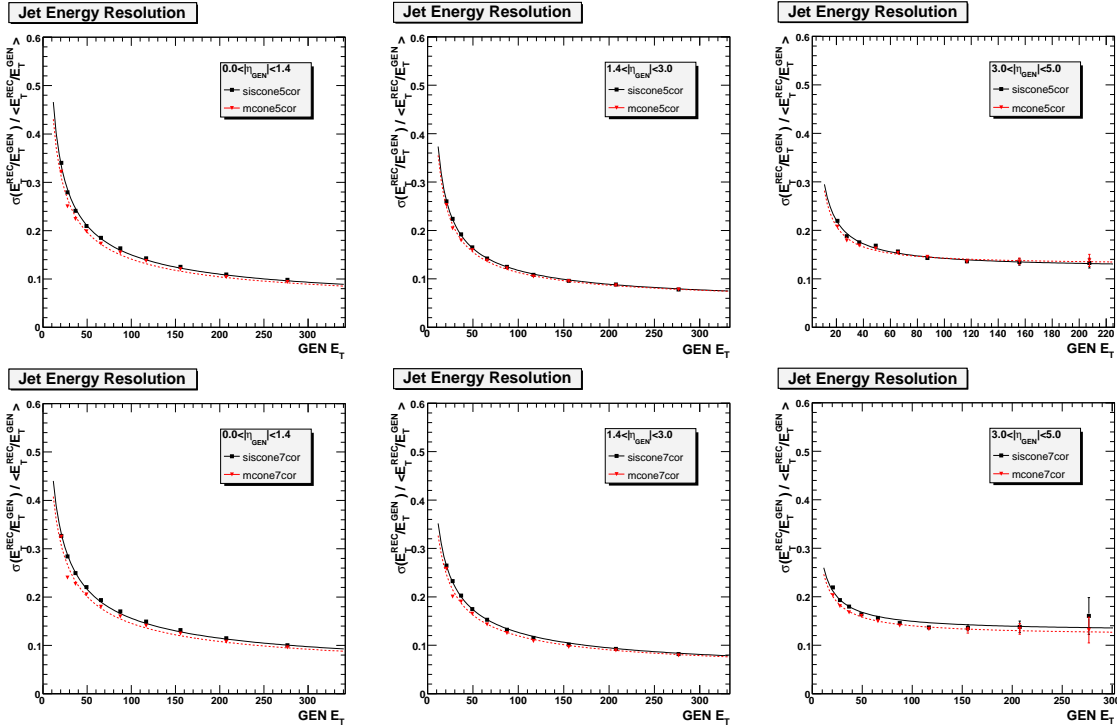


Figure 13: Jet E_T resolution of MidPoint and SIScone for the third leading jet. The top row shows the resolution for jets with a cone of 0.5 and the bottom row is for cone = 0.7. The different columns show the results for different η bins; $|\eta| < 1.4$, $1.4 < |\eta| < 3.0$, and $3.0 < |\eta| < 5.0$.

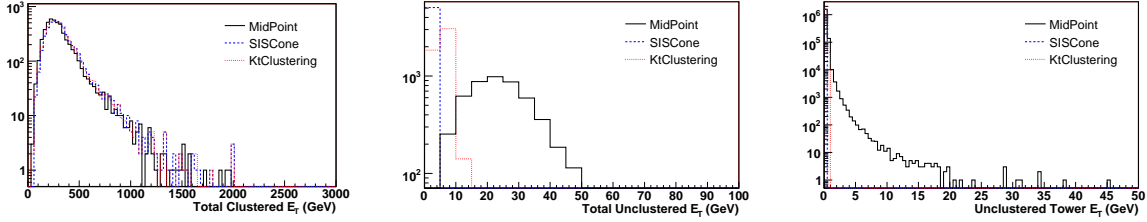


Figure 14: The left plot shows the total E_T of towers clustered in the jets. The middle plot shows the total E_T for towers not included in the jets. The right plot shows the E_T distribution of unclustered towers. A $E_T > 0.5\text{GeV}$ was placed on the towers.

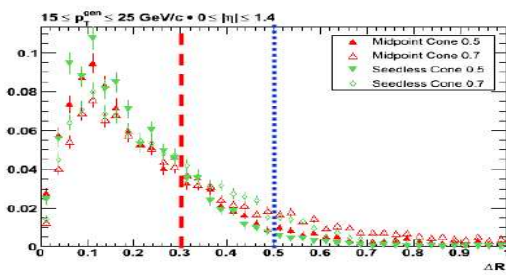


Figure 15: ΔR for jets with $15 < p_T < 25$ and $|\eta| < 1.4$.

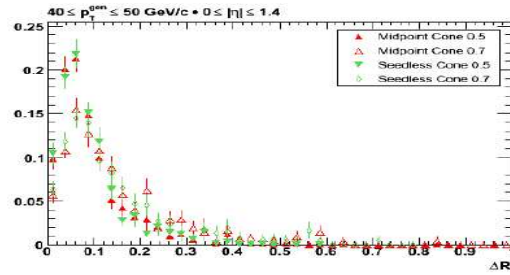


Figure 16: ΔR for jets with $40 < p_T < 50$ and $|\eta| < 1.4$.

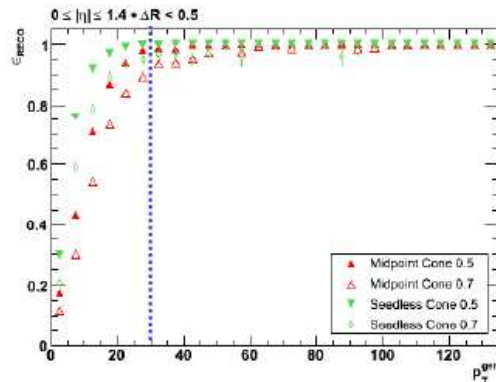
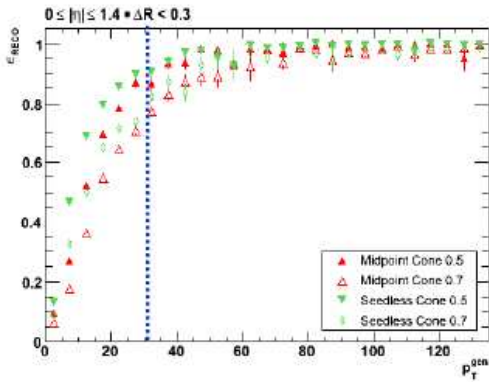


Figure 17: The jet p_T efficiency for $\Delta R < 0.3$ (left) and $\Delta R < 0.5$ (right).

Figure 17 shows the reconstruction efficiency as a function of the jet p_T for $\Delta R < 0.3$ (left) and $\Delta R < 0.5$ (right). As expected the efficiency improves for low p_T as the ΔR requirement is increased. The reconstruction efficiency for SIScone is higher than that of MidPoint.

Figure 18 shows the reconstruction efficiency as a function of the jet rapidity for two different p_T bins.

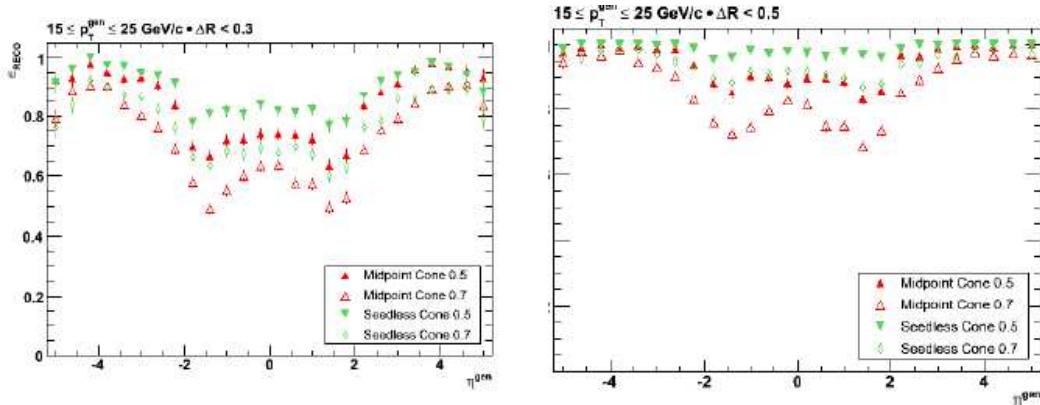


Figure 18: The jet reconstruction efficiency as a function of η for $\Delta R < 0.3$ (left) and $\Delta R < 0.5$.

2.7 Dijet Mass Resolution

The dijet mass resolution depends on both the energy and position of the jet. The resolution was studied using a Z' sample generated with three different masses, 700, 2000, and 5000 GeV using CMSSW 1.6.7. The dijet mass was determined from the two leading jets selected such that they both satisfy $|\eta| < 1.3$. The L2 + L3 factorized corrections was applied as outlined in the WorkBook160JetReco example. The reconstructed dijet mass for GenJet, CaloJet and Corrected CaloJet is shown in Figure 19. The top row shows the results for MidPoint while the bottom row shows the results for SIScone. The results are similar for the two algorithms.

A Gaussian was fit to the distribution in the range from -1.0σ to 1.5σ centered on the mean. The fit procedure was iterated several times starting from the results of the previous fit. The resolution, defined as σ/mean , was then plotted for the three mass points and presented in Figure 20.

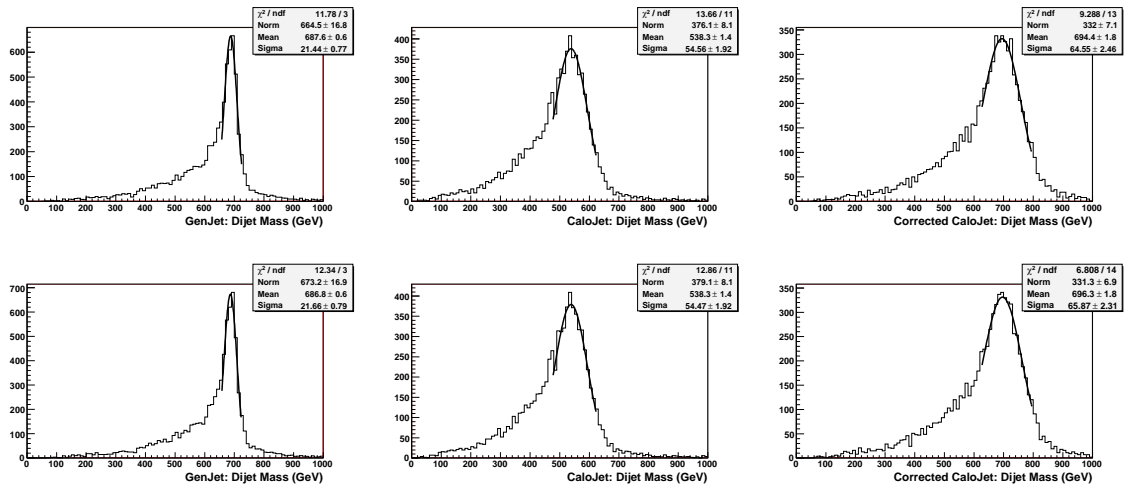


Figure 19: The dijet mass distribution for GenJets, CaloJets, and Corrected CaloJets as determined using MidPoint (top row) and SIScone (bottom row).

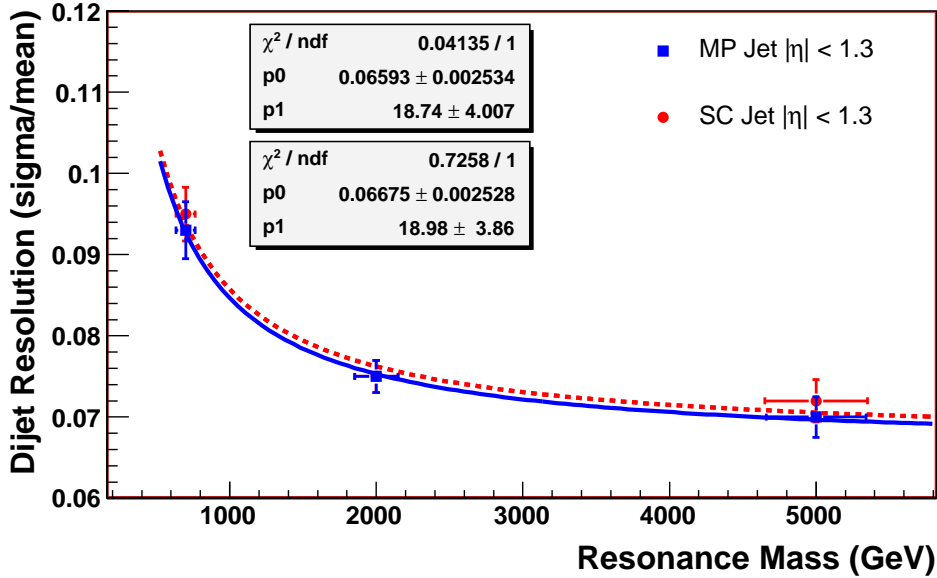


Figure 20: The dijet mass resolution, σ/mean , is plotted as a function of the Z' mass. The resolution obtained for MidPoint and SIS Cone are similar.

2.8 Pileup

The Large Hadron Collider (LHC) will collide protons with an unprecedented instantaneous luminosity of up to $10^{34} \text{cm}^{-2} \text{s}^{-1}$ and a bunch spacing of 25 ns. While this high luminosity is essential for many searches of rare new physics processes at high energy scales, it also complicates analyses, because at each bunch crossing there will be of the order of 20 minimum bias pp interactions, which pollute any interesting hard events with many soft particles. The beams at LHC will have a longitudinal spread, and it may be possible experimentally to associate each charged particle with a distinct primary vertex that corresponds to a single pp interaction and so eliminate some fraction of the soft contamination. However, for neutral particles this is not possible, and most jet measurements are in any case expected to be carried out with calorimeters, which do not have the angular resolution needed to reconstruct the original primary vertex. Therefore kinematic measurements for jets will be adversely affected by pileup (PU). Here we have estimated the effect of pileup which come from by use of two different algorithms Midpoint and SIS Cone.

We have taken a sample of QCD jet events generated with PYTHIA in \hat{p}_T 120-170 GeV, and then passed through the full CMS detector simulation and reconstruction package CMSSW_1_5_2. To simulate additional proton-proton interactions in a beam crossing for in-time PU, the simulated hits (simhits) of signal events were mixed with a random number of minimum bias events in one crossing. The minimum bias events were generated with PYTHIA as inclusive QCD events. The Poission distribution with an average of five and the values corresponding to in-time and out-of-time bunches were taken as zero for simulating in-time PU events.

Figure 21 and Figure 22 shows the shift in jet p_T due to pileup. The shift in jet p_T was calculated from the difference of jet's p_T with and without pileup (being careful to properly match each of the two jets with pileup to the corresponding one without pileup). The shift is significant (up to 25 and 16 GeV for Midpoint and SIS Cone respectively on average) when looking at jets over the entire η region and varies considerably from jet to jet, both because of variation in jet areas and because the pileup fluctuates from event to event. The negative shifts observed for a small subset of jets are attributable to the pileup having modified the clustering sequence, for example breaking one hard jet into two softer subjects. The mean value of shift in jet's p_T due to PU is 0.858 (0.5238) for MidPoint (SIS Cone) when looking at jets over the entire η region. It seems that the jets which are reconstructed from SIS Cone algorithm are less sensitive to PU than with corresponding jets from the Midpoint algorithm.

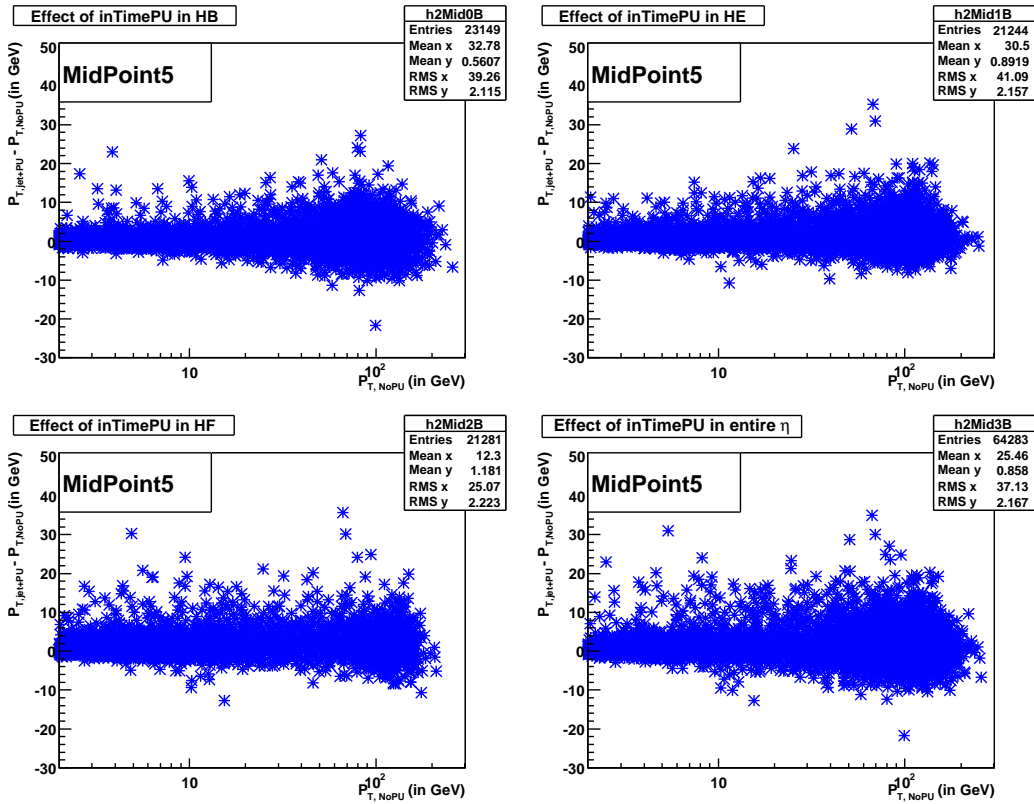


Figure 21: The p_T difference between MidPoint jets with and without pileup is plotted as a function of the jet p_T

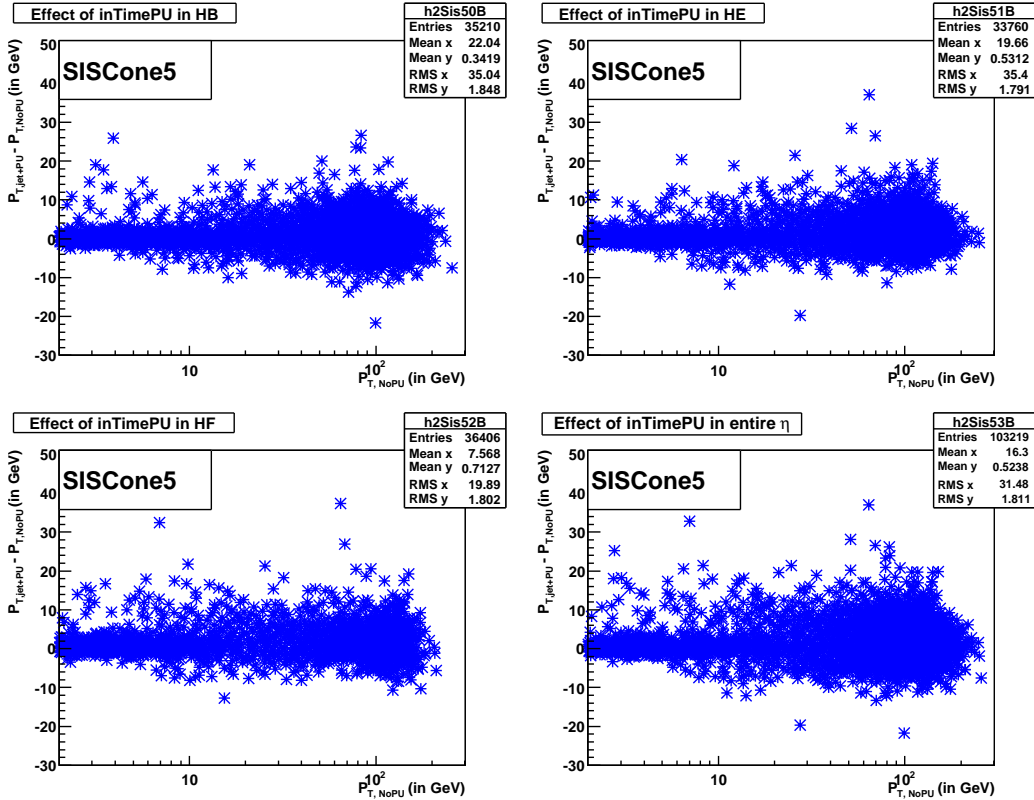


Figure 22: The p_T difference between SISCone jets with and without pileup is plotted as a function of the jet p_T

2.9 Multijet Events

The ability to resolve multijets was studied using 5050 $t\bar{t}$ events (RelVal152TTbar). About 45% or 2280 decay in the fully hadronic mode for which we expect six jets. For this subset of events we count the number of matched jets using the requirement $\Delta R < 0.3$. The minimum ΔR between parton pairs is plotted in Figure 23 on a log scale and shows that most partons are separated by more than $\Delta R > 0.3$. Figure 24 shows the difference between the Reconstructed and Generated ΔR , $\Delta\phi$, $\Delta\eta$, and Δp_T . The different reconstruction algorithm give similar results.

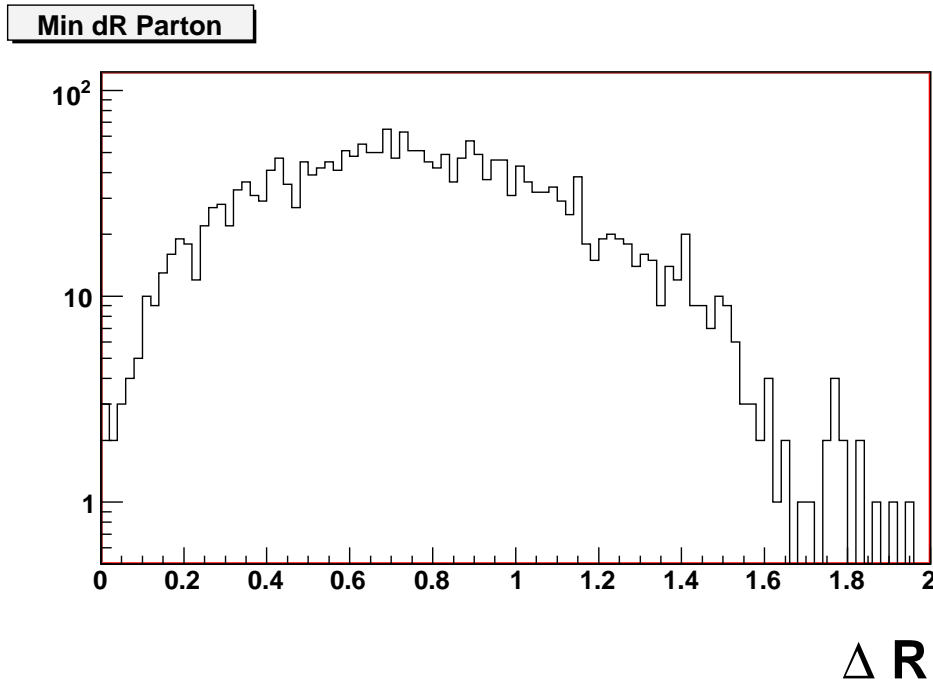


Figure 23: the minimum ΔR between parton pairs for $t\bar{t}$ events. Most partons are separated by more than $\Delta R > 0.3$.

The number of matched jets found by the different algorithms is listed in Table 2

Table 2: Number of matched jets for $t\bar{t}$ events with fully hadronic decay.

Jets	MidPoint	SISCone	KtClus
0	0	1	0
1	0	1	0
2	5	4	0
3	15	18	6
4	89	100	72
5	477	442	399
6	1694	1714	1803
Eff.	74%	75%	79%

2.10 Performance in $t\bar{t}$ Events

The performance of Midpoint and SISCone is compared for $t\bar{t}$ events in which either one (“lepton+jets”) or both (“alljets”) W bosons decay hadronically into a pair of quarks. The ALPGEN MC sample is produced and reconstructed with CMSSW_1.5.2 and does not cover the production of top pairs in association with additional jets (referred to as “ $t\bar{t} + 0$ jets”). After requiring $p_T > 15$ GeV for calorimeter jets, the jet multiplicity, p_T and η distributions are shown in Figure 25 both for Midpoint $R = 0.5$ (top) and SISCone $R = 0.5$ (bottom).

Out of 144775 total lepton+jets events, the number of events with at least four jets satisfying the p_T cut above is

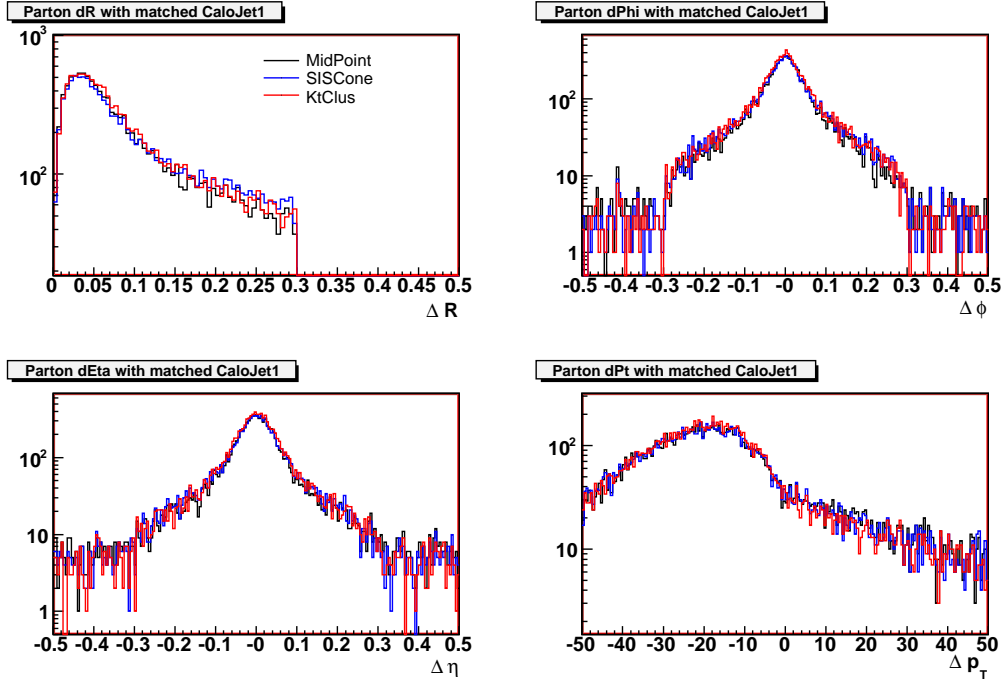


Figure 24: The difference between Calo and Gen reconstructed quantities for matched jets.

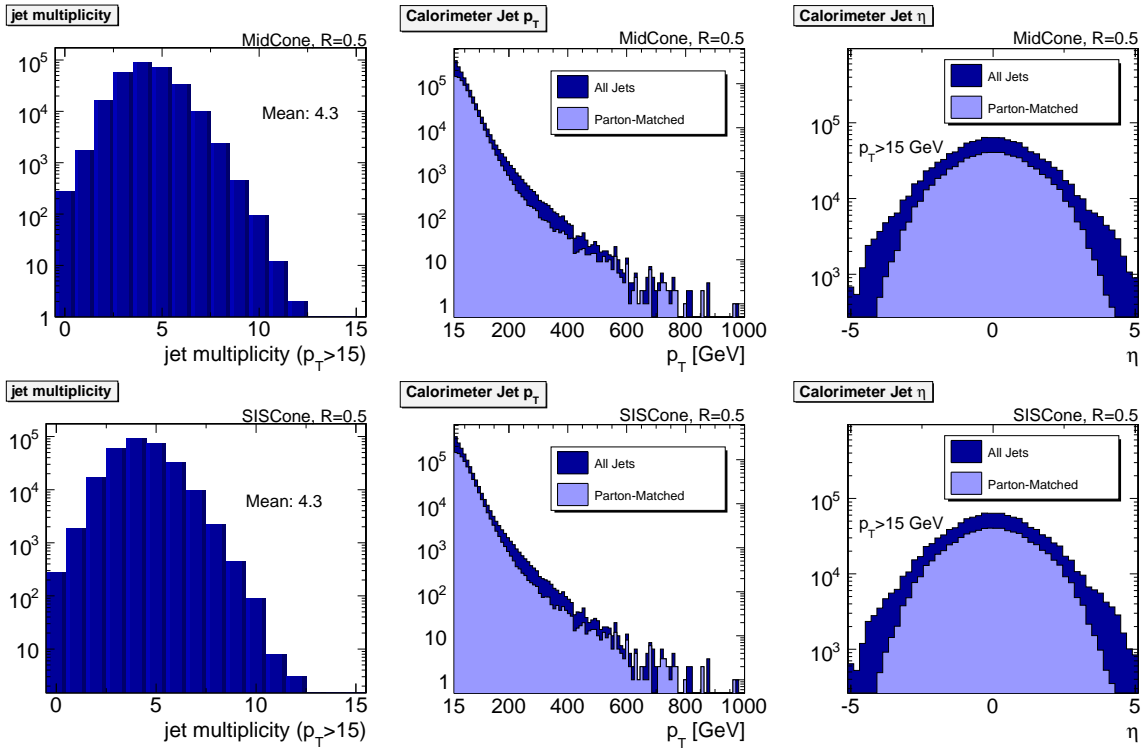


Figure 25: Jet multiplicity (left), p_T (middle), and η (right) distributions for jets reconstructed with Midpoint $R = 0.5$ (top) and SIScone $R = 0.5$ (bottom) in $t\bar{t}$ lepton+jets and alljets events. No attempt is made to remove isolated leptons from the list of jets. The parton distributions for hadronic top decays fully matched to calorimeter jets are also shown.

87966 (60.8 %) for Midpoint and 86736 (59.9 %) for SIScone ($R=0.5$). Of 144800 total alljets events, Midpoint retains 35393 (24.4 %) and SIScone 34499 (23.8 %) events when requiring at least six reconstructed jets with $p_T > 15$ GeV. The efficiency ϵ_{top} is defined as the number of hadronic $t \rightarrow Wb$ decays for which all three quarks in the final state can be matched to calorimeter jets within $\Delta R < 0.5$, divided by all such decays in events which pass the above described jet selection. In lepton+jets events, ϵ_{top} is found to be 16.0 % for Midpoint and 15.8 % for SIScone. ϵ_{top} is determined to be 40.4 % and 40.2 % for Midpoint and SIScone respectively in alljets events, for which $\epsilon_{t\bar{t}}$ is defined additionally as the fraction of events for which both top decays can be matched: 4.5 % for Midpoint, and 4.3 % for SIScone.

The calorimeter jets belonging to fully matched hadronic top decays are used to form dijet (m_W) and three-jet (m_t) masses in order to compare the mass resolution obtained with both algorithms. The resulting mass distributions are shown in Figure 26 for W bosons (left) and top quarks (right) for Midpoint $R = 0.5$ (top) and SIScone $R = 0.5$ (bottom) at several levels of correction: besides generator and calorimeter level distributions, result after application of MCJet energy corrections and additional flavor corrections (“Level-5”) are included as well[?]. The later represents the most accurate level of correction currently available and thus provides the most meaningful measure to compare the resolution obtained with different algorithms. The RMS of the L5-corrected m_W distribution is 13.1 and 13.2 GeV for Midpoint and SIScone reconstructed jets respectively. Similar compatibility is found for the L5-corrected m_t spectra with RMS widths of 22.3 and 22.4 GeV, indicating that both algorithms yield the same mass resolution in $t\bar{t}$ events.

3 Conclusion

The problem of infrared safety arises from applying a minimum p_T requirement in order to define a set of manageable starting seeds. Without the p_T requirement previously used algorithms become too CPU intensive. The MidPoint algorithm, as it is currently being used, has been shown not to be infrared safe to all orders of perturbative calculation. Measurements performed using this algorithm will introduce unnecessary uncertainties when comparing measured results to theory. The SIScone algorithm is infrared safe and the execution time is comparable to MidPoint. The code for the SIScone algorithm is maintained in the external repository, HepForge, and allows different experiments to use exactly the same clustering algorithm. This will help to facilitate the combination and comparison of results from different experiments. The SIScone algorithm has been integrated into CMSSW framework and using the results is as simple as changing the name of the jet collection.

A comparison of reconstructed quantities between MidPoint and SIScone show that the two algorithms have similar results. Jet corrections are available for SIScone and provide the same level of correction as for MidPoint. SIScone has also been shown to be able to perform as well as MidPoint in resolving multijets in $t\bar{t}$ events and yields a comparable mass resolution when reconstructing the top or W . So far no pathologies have been found when using SIScone.

We propose that SIScone be adopted as the default cone-based jet algorithm at CMS and added to the standard reconstruction sequence. In order to reduce confusion and overhead it is recommended that MidPoint be dropped from the reconstruction sequence but maintained so that it can be called by the user.

References

- [1] **JHEP 05 (2007) 086**, G.Soyez and G.Salem, “A practical Seedless Infrared-Safe Cone jet algorithm”.
- [2] <http://projects.hepforge.org/siscone/>
- [3] Midpoint
- [4] Kt Clustering
- [5] Fast Jet
- [6] **CMS IN-2007/053**, M.Vazquez Acosta et al., Jet and MET Performance in CMSSW_1_2_0,

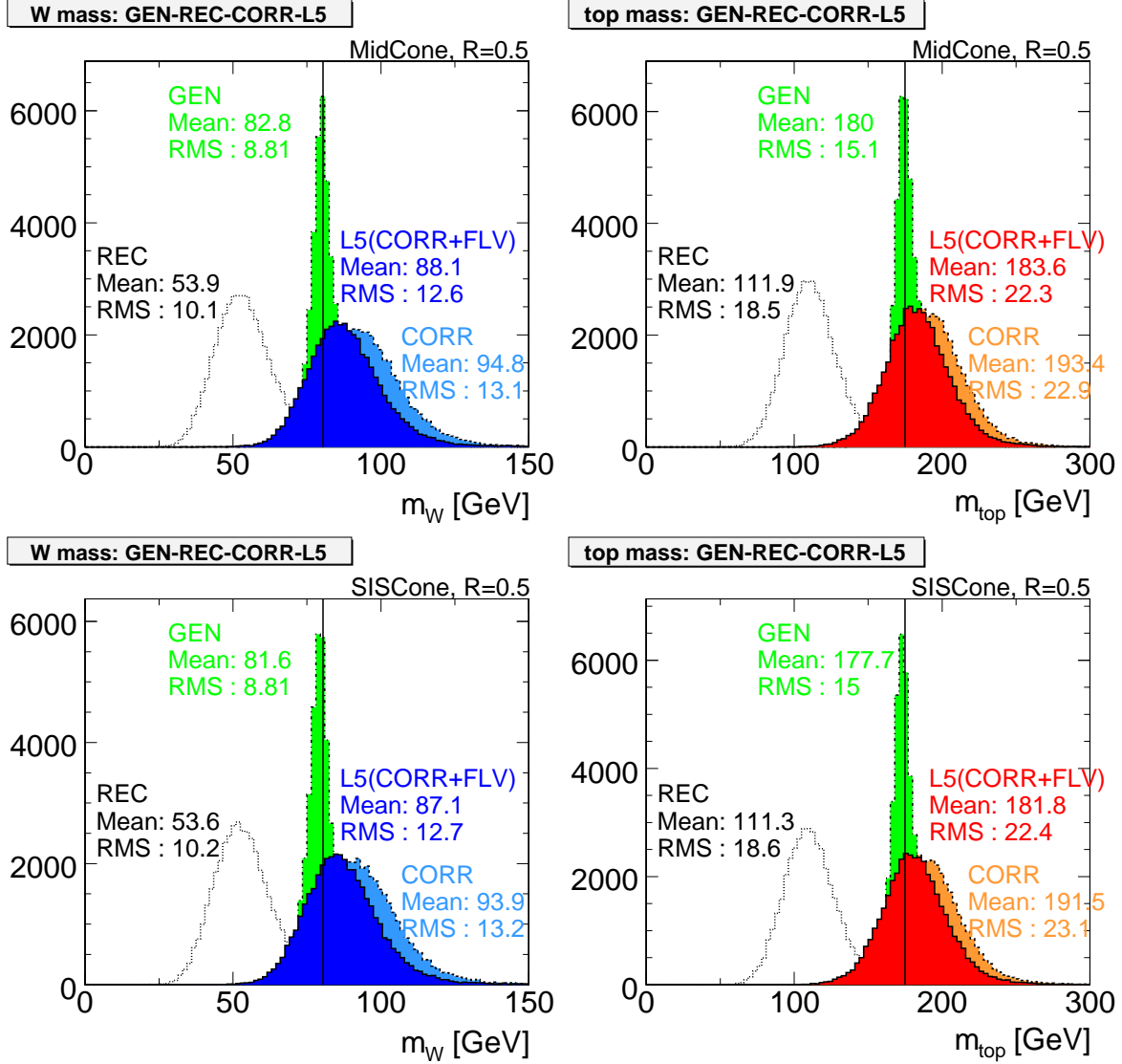


Figure 26: m_W (left) and m_t (right) distributions for hadronic top quark decays reconstructed with Midpoint $R = 0.5$ (top) and SIScone $R = 0.5$ (bottom). Four different correction levels are shown: particle-level (“GEN”), calorimeter-level (“REC”), MCJet-corrected calorimeter-level (“CORR”), and “Level-5”, which accounts for the flavor dependence of the MCJet jet energy correction. The black vertical lines indicate the generated W boson and top quark mass of 80.42 GeV and 175 GeV respectively.